reported, whereas for $Cr_2(O_2CNH_2)_4$ it was found that while all other MO energies decreased slightly, relative to those in $Cr_2(O_2CH)_4$, the energy of the δ orbital rose. The net effect was that the $\delta-\delta^*$ orbital gap decreased from ca. 0.6 eV in $Cr_2(O_2CH)_4$ to ca. 0.1 eV in $Cr_2(O_2CNH_2)_4$. While we do not propose to make a quantitative comparison to the experimental S-T data, it is clear that the calculated effect is qualitatively correct and is of about the right magnitude.

Conclusion

While $Cr_2(O_2CR)_4L_2$ compounds can be (and presumably usually are) contaminated by paramagnetic impurities (most likely Cr(III) species arising by oxidative decomposition), they also have inherent paramagnetism owing to the existence of a low-lying triplet state. The S-T gap is an inverse function of the Cr-Cr distance but also can be markedly affected by changing the nature of the ligands, e.g., from RCO_2^- to $R_2NCO_2^-$. A good, but not conclusive, case may be made that the two states (and the principal contributing configurations) that define the S-T gap are $^1A_{1g}$ ($\sigma^2\pi^4\delta^2$) and $^3A_{2u}$ ($\sigma^2\pi^4\delta\delta^*$).

Acknowledgment. We thank the National Science Foundation for financial support and Dr. Chris James for advice on fitting the NMR data. We also thank Prof. Carlos A. Murillo for the sample of $Cr_2(O_2CCF_3)_4(Et_2O)_2$ and Prof. Fausto Calderazzo for that of $Cr_2(O_2CNEt_2)_4(NEt_2H)_2$.

Redox-Active Crown Ethers. Electrochemical and Electron Paramagnetic Resonance Studies on Alkali Metal Complexes of Quinone Crown Ethers

Milagros Delgado,[†] Robert E. Wolf, Jr.,[‡] JudithAnn R. Hartman,[†] Gillian McCafferty,[†] Rahmi Yagbasan,[§] Simon C. Rawle,[†] David J. Watkin,[§] and Stephen R. Cooper*,[†]

Contribution from the Inorganic Chemistry Laboratory, University of Oxford, Oxford OX1 3QR, England, Chemical Crystallography Laboratory, University of Oxford, Oxford OX1 3PD, England, and Department of Chemistry, Harvard University, Cambridge, Massachusetts 02138.
Received March 20, 1992

Abstract: Structural studies on [M(NCS)·(5QC-HQDME)] (M = Li, Na) as well as free 6QC-HQDME and [M(NCS)·(6QC-HQDME)] (M = Na, K) (where 5QC-HQDME is 15,17-dimethyl-16,18-dimethoxy-3,6,9,12-tetraoxabicyclo-[12.3.1]octadeca(1,14,16)triene, and 6QC-HQDME is 15,17-dimethyl-16,18-dimethoxy-3,6,9,12,15-pentaoxabicyclo-[15.3.1]heneico(1,14,16)triene) show that in all cases the metal ion binds to the anisole oxygen atom in the 1-position. Only in the case of [K(NCS)·(6QC-HQDME)] do both benzylic O atoms bind to the metal ion; in the other complexes only one of these O atoms interacts with M^+. In each complex all of the non-benzylic crown O atoms coordinate. These results indicate that the benzylic O atoms contribute suboptimally to complexation. Crystallographic data are as follows: [Li(NCS)·(5QC-HQDME)], monoclinic, $C_{19}H_{28}NO_6SLi$, space group $P2_1/n$, a = 14.103 (4) Å, b = 8.493 (4) Å, c = 19.128 (8) Å, β = 108.70 (9)°, Z = 4; [Na(NCS)·(5QC-HQDME)], monoclinic, $C_{19}H_{28}NO_6SNa$, space group $P2_1/c$, a = 10.182 (4) Å, b = 8.601 (1) Å, c = 25.631 (3) Å, β = 97.29 (3)°, Z = 4; 6QC-HQDME, orthohombic, $C_{20}H_{32}O_7$, space group $P2_12_12_1$, a = 8.195 (1) Å, b = 11.541 (1) Å, c = 22.449 (3) Å, Z = 4; [Na(NCS)·(6QC-HQDME)]·MeCN, monoclinic, $C_{23}H_{35}N_2O_7SNa$, space group $P2_1/c$, a = 11.308 (1) Å, b = 14.521 (2) Å, c = 16.440 (4) Å, β = 91.56 (1)°, Z = 4; [K(NCS)·(6QC-HQDME)], monoclinic, $C_{21}H_{32}NO_7SK$, space group $P2_1/c$, a = 17.377 (3) Å, b = 10.600 (2) Å, c = 27.538 (7) Å, β = 102.41 (3)°, Z = 8. Electrochemical and EPR studies show that redox-active crown ethers incorporating quinone groups successfully couple ion binding by the crown ether to the redox state of the quinone group. Alkali metal ions cause potential shifts that establish-differential redox-induced complexation that qualitatively and quantitatively differs from ion-pairing effects. They also perturb the EPR hyperfine splittings in the semiquinone moieties in a characteristic fashion, as well as in one case giving rise to ^{23}Na superhyperfine splitting.

Introduction

Coupled reactions play an essential role in biology. According to the chemiosmotic hypothesis,[1] energy transduction occurs by coupling discharge of a pH gradient to synthesis of ATP, hydrolysis of which, in turn, drives formation of ion concentration gradients across membranes.[2] Metabolic pathways drive endothermic reactions by coupling them to other highly exothermic processes.

Outside of biology, coupled reactions most commonly arise from the intrinsic properties of the reactants, and not by design. In a prosaic example, proton displacement upon coordination of a ligand to a metal couples these two reactions; manipulation of pH then influences metal ion binding, and vice versa. In few cases, however, has one reaction been intentionally coupled to another *to which it bears no intrinsic relationship* (as opposed to the example above).

Redox-active crown ethers such as I represent one such case of intentional coupling. In suitably designed molecules the proximity of the crown loop to a reducible moiety effectively couples ion binding and redox reactivity, phenomena that would not perturb each other were the two functional groups contained in different molecules.

Quinones offer several advantages as the electroactive component for two reasons. First, they have been thoroughly studied by electrochemical and EPR methods. Second, an obvious but important point, reduction yields the anionic semiquinone; on electrostatic grounds a neutral/anionic couple should yield higher

[†] Inorganic Chemistry Laboratory.
[‡] Harvard University.
[§] Chemical Crystallography Laboratory.
* To whom correspondence should be addressed at the Inorganic Chemistry Laboratory, University of Oxford.

(1) Mitchell, P. *Nature (London)* **1961**, *191*, 144-148.
(2) Racker, E. *Acc. Chem. Res.* **1979**, *12*, 338-344.

0002-7863/92/1514-8983$03.00/0

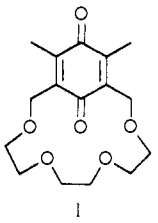

I

stability constants than those afforded by neutral/cationic couples. Initial reports on redox-active crown ethers[3-8] have been followed by a substantial body of work,[9] with quinone-based systems receiving particularly extensive investigation.[10-20]

In addition to their conceptual importance, redox-active crowns have obvious applications in the design of sensor systems.[21] Redox-active crown ethers also attract interest for use in electrochemically-driven ion transport[14,22] and possibly as functional analogues of macrocyclic quinoid antibiotics such as macbecin.[23]

This paper reports structural, electrochemical, and EPR spectroscopic studies of quinone crown ethers with alkali metal cations that establish that coupling has been successfully achieved. To examine the structural basis of the coupling we have undertaken the diffraction studies reported here. Structural investigation of quinone crown complexes reveals the source of the coupling between ion binding and redox reactions: a strong M–O(quinoid) bond. (Here and throughout the paper "quinoid" is taken to include the hydroquinone dimethyl ether as a model for the M···O interactions that occur with the corresponding quinone and semiquinone.) It also shows that the quinoid group pivots to accommodate different metal ions, and that therefore efforts to improve selectivity must focus upon conformationally "stiffening" the crown loop.

Experimental Section

All solvents were distilled under nitrogen and stored over molecular sieves; dichloromethane and acetic anhydride were distilled from phosphorus pentoxide, and THF from sodium/benzophenone. Pentane was dried by storing over sodium wire. Alkali metal thiocyanate salts were dried in vacuo at 45 °C for 2 d and subsequently stored under an atmosphere of nitrogen. Most other reagents were supplied by Aldrich Chemical Co. and used without prior purification. Elemental analyses were performed by Mr. Mervyn Gascoyne, Mr. Jim Kench, and Ms. Ann Douglas of the microanalytical service of the Inorganic Chemistry Laboratory. Analytical thin-layer chromatography was carried out on micro blend 41 silica gel plates with spots made visible with iodine vapor. Column chromatography was performed on 70–230 mesh silica gel (Aldrich). Dimethylformamide (DMF) was stirred overnight over BaO, decanted, distilled under reduced pressure, and stored under nitrogen over 4 Å molecular sieves. All solutions were prepared under an atmosphere of dry N_2. Tetraethylammonium tetrafluoroborate (Fluka) was dried in vacuo overnight and stored in a desiccator. Alkali metal tosylate salts were prepared from the reaction of the alkali metal carbonate salts with *p*-toluenesulfonic acid. They were dried in vacuo at 45 °C over silica gel overnight and stored in a desiccator.

Infrared spectra were recorded on a Perkin-Elmer 55R Fourier transform spectrometer, while a Bruker AM300 or a Varian HFT-80 NMR spectrometer was used to record ^{1}H NMR spectra. Spectra were all determined in deuteriochloroform and residual protons used as internal reference. Mass spectra were measured by C. J. Botham of the Inorganic Chemistry Laboratory, Oxford, on a AEI MS9 02 mass spectrometer.

Cyclic voltammetry was performed at room temperature under N_2 on DMF solutions containing 0.1 M electrolyte ($Et_4N\,BF_4$, $Et_4N\,BPh_4$, or $M^+{}^-OTs$) and the electroactive species at millimolar concentrations. (For Rb^+ the tetraphenylborate salt was used instead of the tosylate owing to its greater solubility.) A Pt disk was used as the working electrode and a Pt wire as the counterelectrode. Potentials are reported vs saturated calomel electrode (SCE). The measurements were performed on a Princeton Applied Research 175 programmer and a 173 potentiostat with IR compensation.

Electron paramagnetic resonance spectra were recorded on DMF solutions of the semiquinones (generated by controlled-potential electrolysis in the cavity) with a Bruker ESP-300 spectrometer at X-band. A quartz flat cell was used for the experiments with an Hg pool working electrode. The potential was controlled between −0.9 and −1.7 V with a Solatron PSU Model AS1411.2 constant voltage supply.

Synthesis of Compounds. (a) 2,6-Dimethylbenzoquinone. A solution of sodium nitrite (34 g, 0.50 mol) in water (100 mL) was cooled in an ice bath. Chopped ice (200 g) was added and the solution stirred steadily during the addition of fresh sodium metabisulfite solution (100 mL 35% w/v), followed by addition of glacial acetic acid (20 mL). The reaction is completed in 3 min when 25 mL of concentrated ammonia (sp gr 0.80) are added. Potassium permanganate (12.6 g, 0.079 mol) in 400 mL of water was then added to the solution over 1 h to give a dark brown solution. The mixture was stirred for an additional 10 min and then filtered by gravity to remove precipitated manganese dioxide. The purple filtrate (total volume approximately 1.5 L) was poured with stirring into a saturated KCl aqueous solution to precipitate the Fremy's salt as an orange solid. The salt was filtered, weighed, and immediately dissolved in water at 0 °C. To this stirred purple solution was added slowly 2,6-dimethylphenol (4.5 g, 0.037 mol) in 500 mL of methanol at room temperature. The resulting yellow solution was extracted with dichloromethane ($3 \times {}^1/_5$ volume), washed (brine, 100 mL), dried (Na_2SO_4), and concentrated to yield a yellow solid that after sublimation gave bright yellow needles (4.2 g, 83%). Mp: 70–71 °C (lit.[13] mp 71–72 °C). NMR (300 MHz, $CDCl_3$): 6.56 ppm (s, 2 H, ArH), 2.06 (s, 6 H, CH_3). IR (Nujol) cm^{-1}: 2922 w, 2854 w, 1651 s, 1614 s, 1462 m, 1377 m, 1316 m, 1290 m, 1206 m, 1181 m, 1036 s, 918 m, 855 w, 794 m.

(b) 2,6-Dimethylhydroquinone was prepared from 2,6-dimethylquinone by the method of Smith and Opie.[24] A solution of 2,6-dimethylquinone (8.87 g, 65 mmol) dissolved in acetic acid (45 mL) and water (28 mL) was added to zinc (15.0 g, 30 mesh). The resulting orange solution was allowed to reflux for 2 h, before boiling water (25 mL) was added to the reaction mixture and the pale yellow solution decanted from the unreacted zinc. The zinc mesh was further washed with boiling water (25 mL), and the combined washings were cooled in an ice bath for 30 min to yield white crystals that were filtered off, washed with cold water, and dried in vacuo (7.35 g, 81%). MP 147–48 °C; *m/e* 138.37. NMR (300 MHz, $CDCl_4$): 6.5 (s, 2 H, Ar-H), 4.55 (d, 2 H, OH), 2.2 (s, 6 H, CH_3). IR (Nujol) cm^{-1}: 3600–2200 bs, 1660 w, 1456 s, 1397 w, 1330 s, 1258 m, 1151 s, 1063 w, 965 m, 896 s, 878 m, 784 s.

(c) 2,6-Dimethylhydroquinone Dimethyl Ether. To a suspension of NaH (720 mg, 60% oil dispersion, washed with hexane, in 20 mL of dry THF) in a Schlenk flask under N_2 was added via cannula 2,6-dimethylhydroquinone (1.24 g, 9 mmol) in 10 mL of dry THF, followed by MeI (5.12 mL, 36 mmol), and the resulting mixture was brought to reflux to give a blue solution. After 12 h of reflux the now beige solution was stripped of solvent and redissolved in Et_2O/H_2O (20/5 mL). The compound was extracted with Et_2O (3 × 25 mL), and the combined organic layers were washed with H_2O (25 mL), dried over anhydrous

(3) Sugihara, K.; Kamiya, H.; Yanaguchi, M.; Kaneda, T.; Misumi, S. *Tetrahedron Lett.* **1981**, 1619–1622.
(4) Kaifer, A.; Echegoyen, L.; Gokel, G. W.; Goli, D. M.; Gustowski, D. A. *J. Am. Chem. Soc.* **1983**, *105*, 7168–7169.
(5) Hammond, P. J.; Bell, A. P.; Hall, C. D. *J. Chem. Soc., Perkin Trans. 1* **1983**, 707–715.
(6) Beer, P. D.; Hammond, P. J.; Hall, C. D. *J. Chem. Soc., Chem. Commun.* **1983**, 1161–1163.
(7) Bock, H.; Hierholzer, B.; Voegtle, F.; Hollmann, G. *Angew. Chem., Int. Ed. Engl.* **1984**, *23*, 57–58.
(8) Wolf, R. E.; Cooper, S. R. *J. Am. Chem. Soc.* **1984**, *106*, 4646–4647.
(9) Beer, P. D. *Chem. Soc. Rev.* **1989**, *18*, 409–450.
(10) Bock, H.; Hierholzer, B.; Schmalz, P. *Angew. Chem., Int. Ed. Engl.* **1987**, *26*, 791–793.
(11) Bock, H.; Herrmann, H. F. *J. Am. Chem. Soc.* **1989**, *111*, 7622–7624.
(12) Delgado, M.; Echegoyen, L.; Gokel, G. W.; Gustowski, D. A.; Gatto, V. J.; Yoo, H. K. *J. Am. Chem. Soc.* **1988**, *110*, 119–124.
(13) Dietl, F.; Gierer, G.; Merz, A. *Synthesis (Stuttgart)* **1985**, 626–631.
(14) Echegoyen, L. E.; Yoo, H. K.; Gatto, V. J.; Gokel, G. W.; Echegoyen, L. *J. Am. Chem. Soc.* **1989**, *111*, 2440–2443.
(15) Gustowski, D. A.; Delgado, M.; Echegoyen, L.; Gatto, V. J.; Gokel, G. W. *J. Am. Chem. Soc.* **1986**, *108*, 7553–7560.
(16) Hall, C. D.; Nyburg, S. C.; Parkins, A. W.; Speers, P. *J. Chem. Soc., Chem. Commun.* **1989**, 1730–1732.
(17) Hayakawa, K.; Kido, K.; Kanematsu, K. *J. Chem. Soc., Perkin Trans.* **1988**, 511–519.
(18) Ossowski, T.; Schneider, H. *Chem. Ber.* **1990**, *123*, 1673–1677.
(19) Togo, H.; Hashimoto, K.; Kikuchi, O.; Morihashi, K. *Bull. Chem. Soc. Jpn.* **1988**, *61*, 3026–3028.
(20) Glezer, V. T.; Kolesnikov, V. T.; Kartoflitskaya, A. P.; Stradyn, Y. P. *Zh. Obsh. Khim.* **1988**, *58*, 2377–2383.
(21) Janata, J. *Anal. Chem.* **1990**, *62*, 33R–44R.
(22) Saji, T.; Kinoshita, I. *J. Chem. Soc., Chem. Commun.* **1986**, 716–717.
(23) Muroi, M.; Haibara, K.; Asai, M.; Kamiya, K.; Kishi, T. *Tetrahedron* **1981**, *37*, 1123–1130.
(24) Smith, L. I.; Opie, J. W. *J. Am. Chem. Soc.* **1941**, *63*, 937–940.

Scheme I

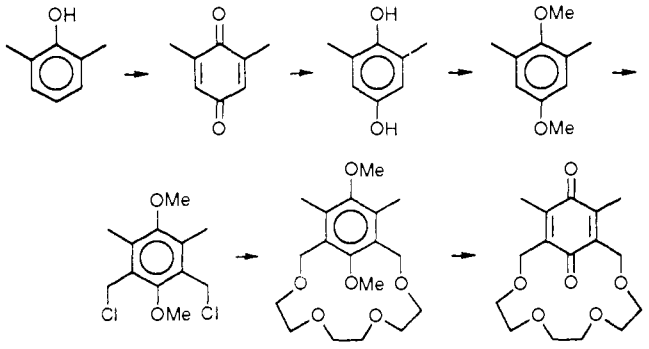

sodium sulfate, and concentrated to give an orange oil, which upon column chromatography (SiO_2, CH_2Cl_2) yielded 1.24 g (83%) of a yellow-orange oil. NMR (300 MHz, $CDCl_3$): 6.57 (s, 2 H, Ar-H), 3.76 (s, 3 H, O-CH_3), 3.69 (s, 3 H, O-CH_3), 2.28 (s, 6 H, CH_3). IR (Nujol) cm^{-1}: 2939 w, 2836 m, 1652 m, 1597 s, 1487 s, 1420 w, 1375 m, 1326 s, 1263 s, 1221 w, 1194 m, 1150 s, 1092 s, 1066 m, 1014 m, 938 m, 855 w, 811 w, 758 w, 737 w.

(d) 3,5-Dichloromethyl-2,6-dimethylhydroquinone Dimethyl Ether. A mixture of 2,6-dimethylhydroquinone (0.5 g, 3.0 mmol) and paraformaldehyde (0.288 g, 1.74 mmol) in 1.88 mL of concentrated HCl was refluxed for 24 h, during which time a waxy solid deposited. The orange/brown mixture was extracted with dichloromethane (40 mL) and washed with water (20 mL) and then with brine (2 × 20 mL). The organic extracts were dried over sodium sulfate and concentrated to a white/brown residue. Flash chromatography on a silica gel column with dichloromethane as eluent yielded the pure product as a pale yellow solid. Recrystallization from hexane gave white needle-like crystals: yield 0.41 g (52%); TLC (silica gel, CH_2Cl_2) R_f 0.70; mp 137.5–138.5 °C; parent ion peak at 261; NMR (300 MHz, $CDCl_3$) 4.70 (s, 4 H, Ar-CH_2–), 3.95 (s, 3 H, OCH_3), 3.67 (s, 3 H, –OCH_3), 2.33 (s, 6 H, –CH_3); IR (KBr) cm^{-1} 3400 w, 2920 w, 2370 w, 1600 w, 1450 s, 1400 m, 1280 s, 1257 s, 1242 s, 1186 w, 1170 w, 1154 w, 1112 w, 1062 s, 998 s, 963 w, 915 w, 850 w, 804 m, 725 m, 662 m, 640 m. Anal. Calcd for $C_{12}H_{16}Cl_2$: C, 54.77; H, 6.07; Found: C, 54.76; H, 5.74.

(e) 2,6-Bis(methoxymethyl)-3,5-dimethylhydroquinone Dimethyl Ether. To 3,5-dichloromethyl-2,6-dimethylhydroquinone dimethyl ether (0.2 g, 76 mmol) dissolved in 4 mL of dry THF was added a methanolic solution of NaOMe (prepared by addition of Na metal (74 mg, 3.2 mmol) to 7 mL of MeOH). The mixture was refluxed for 1.5 h, filtered, concentrated, and then washed with H_2O (2 × 10 mL) and then brine (2 × 10 mL), dried over Na_2SO_4, and evaporated to yield an off-white solid that was recrystallized from hexane: yield 0.165 g (85%); TLC (silica gel, CH_2Cl_2) R_f 0.15. NMR (300 MHz, $CDCl_3$) 4.48 (s, 4 H, Ar-CH_2–), 3.78 (s, 3 H, –OCH_3), 3.66 (s, 3 H, –OCH_3), 3.42 (s, 6 H, –OCH_3), 2.32 (s, 6 H, –CH_3); IR (KBr) cm^{-1} 2870 w, 2050–1900 bw, 1590 m, 1435 s, 1360 s, 1240 s, 1180 m, 1130–1010 bs, 987 s, 934 s, 830–785 bw, 775 w, 718 m. Oxidation by the AgO method described below affords the corresponding quinone.

(f) 5QC-HQDME (1). Quinone crowns and their hydroquinone dimethyl ethers were synthesized by the route shown in Scheme I. To a refluxing suspension of sodium hydride (1.2 g, 30 mmol of a 60% oil dispersion that had been washed with dry pentane) in dry THF (200 mL) under a nitrogen atmosphere was added a solution of 2,6-bis(chloromethyl)-3,5-dimethylhydroquinone dimethyl ether (2.47 g, 9.4 mmol) and triethylene glycol in THF (75 mL) over a period of 16 h. The reaction mixture was then refluxed for an additional hour and cooled to room temperature, and then water (5 mL) was added to quench excess sodium hydride. The solvent was removed in vacuo and the resulting yellow residue redissolved in water (40 mL) and dichloromethane (75 mL). The organic phase was separated, washed with water (25 mL), and dried over anhydrous sodium sulfate and the solvent was removed to produce a viscous, yellow oil. Flash chromatography on a silica gel column with diethyl ether/ethyl acetate (4:1 v/v) as an eluent yielded the product as a white solid (1.4 g, 44%); *m/e* 340. NMR (300 MHz, $CDCl_3$): 4.60 (s, 4 H, Ar-CH_2–), 3.80 (s, 3 H, OCH_3), 3.78 (s, 3 H, OCH_3), 3.60–3.45 (m, 12 H, –OCH_2CH_2O–), 2.30 (s, 6 H, CH_3). The same route with higher oligoethylene glycols yielded the corresponding homologous 6QC-HQDME (47%), 7QC-HQDME (33%), and 8QC-HQDME (24%).

(g) 6QC-HQDME (2). *m/e* 384; mp 102–103 °C. NMR (60 MHz, $CDCl_3$): 4.65 (s, 4 H, Ar-CH_2–), 4.0 (s, 3 H, O-CH_3), 3.80 (s, 3 H, O-CH_3), 3.60–3.45 (m, 16 H, –OCH_2CH_2O–), 2.30 (s, 6 H, CH_3). IR (Nujol) cm^{-1}: 2924 s, 1600 w, 1461 s, 1404 m, 1347 s, 1259 s, 1180–1050 bs, 1012 m, 945 m, 892 m, 836 w, 796 w, 723 s. Anal. Calcd for $C_{20}H_{32}O_7$: C, 62.4; H, 8.4. Found: C, 62.3; H, 8.3.

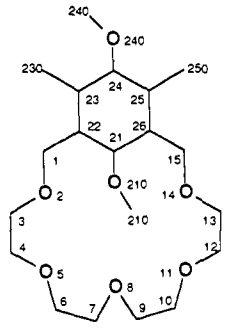

Figure 1. Structure of 6QC-HQDME (I) showing the atomic numbering scheme.

(h) 7QC-HQDME (3). *m/e* 428. NMR (80 MHz, $CDCl_3$): 4.55 (s, 4 H, Ar-CH_2–), 3.91 (s, 3 H, O-CH_3), 3.66 (s, 3 H, O-CH_3), 3.70–3.50 (m, 20 H, –OCH_2CH_2O–), 2.31 (s, 6 H, CH_3); IR (liquid) cm^{-1}: 2899 s, 1742 w, 1610 w, 1486 s, 1464 s, 1403 m, 1370 w, 1347 w, 1235 s, 1163–1053 bs, 1035 w, 1011 m, 991 w, 840 m, 768 w, 733 m, 699 w.

(i) 8QC-HQDME (4). *m/e* 472. NMR (80 MHz, $CDCl_3$): 4.58 (s, 4 H, Ar-CH_2–), 3.85 (s, 3 H, O-CH_3), 3.67 (s, 3 H, O-CH_3), 3.71–3.55 (m, 24 H, –OCH_2CH_2O–), 2.31 (s, 6 H, CH_3). IR (liquid) cm^{-1}: 2872 s, 1742 w, 1605 w, 1480 s, 1460 s, 1401 m, 1372 w, 1320 m, 1242 m, 1160–1050 bs, 1030 w, 1008 m, 990 w, 851 m, 765 w, 730 m, 695 w.

(j) Quinone crowns 5QC–8QC. 5QC–8QC were prepared (72–95% yield) from the corresponding hydroquinone dimethyl ethers by the oxidative demethylation method of Snyder and Rapoport.[25] In a typical reaction 6QC was prepared by dissolving 79 mg (2.05 × 10^{-4} mol) of 6QC-HQDME in 2 mL of 1,4-dioxane (passed through activated alumina) and adding AgO (151 mg, 1.23 mmol), and then the solution was stirred until a fine suspension of AgO formed. Nitric acid (0.19 mL of 6 N HNO_3) was added slowly and the solution stirred until all the AgO was consumed (2 min). The reaction was quenched with CH_2Cl_2/H_2O (8/2 mL), and the organic phase was separated, washed with water (2 mL), dried over Na_2SO_4, and concentrated to give a bright yellow oil which was further purified by flash chromatography using ethyl acetate–diethyl ether (4:1 v/v) as eluent to yield 6QC as a bright yellow oil (72%). NMR (300 MHz, $CDCl_3$): 4.37 (s, 4 H, Ar-CH_2–), 3.4–3.6 (m, 20 H, –OCH_2CH_2O–), 2.05 (s, 6 H, CH_3).

(k) [Na(NCS)·(1)]. A mixture of **1** (291 mg, 0.76 mmol) and NaNCs (62 mg, 0.76 mmol) was refluxed in dry tetrahydrofuran until both had dissolved (approximately 10 min). Evaporation of the reaction mixture in vacuo yielded a yellow solid, which upon recrystallization from tetrahydrofuran gave diffraction quality crystals. Analysis: Found (calcd for $C_{19}H_{28}NO_6SNa$): C, 53.7 (54.14); H, 6.8 (6.70); N, 3.45 (3.32). IR: ν_{CN} 2060 cm^{-1}. Density (measured by flotation in hexane/CCl_4) 1.26 g cm^{-1}. Analogous procedures afforded the corresponding LiNCS and KNCS complexes.

(l) [Li(NCS)·(1)]. Anal. Found (calcd for $C_{19}H_{28}NO_6SLi$): C, 56.5 (56.29); H, 7.1 (6.96); N, 3.4 (3.45). IR: ν_{CN} 2060 cm^{-1} (s). Density (measured by flotation in hexane/CCl_4) 1.25 g cm^{-1}.

(m) [Na(NCS)·(2)]·MeCN. The above procedure gave the unsolvated complex. Anal. Found (calcd for $C_{22}H_{34}N_1O_7SNa$): C, 54.7 (54.18); H, 7.0 (6.93); N, 2.8 (3.01). Recrystallization from acetonitrile gave diffraction quality crystals of the acetonitrile solvate (IR: ν_{CN} 2060 cm^{-1}).

X-ray Crystallography. General Procedures. A single crystal sealed in a glass capillary was mounted in a Nicolet or Enraf Nonius CAD4 diffractometer containing either a Cu or Mo X-ray source. Data-collection parameters appear in Table I. Three standard reflections were measured every hour; data were corrected for decomposition, if any. Crystallographic calculations were performed on a VAX 11/750 computer with the CRYSTALS package of programs. The structures were solved by direct methods (SHELX), and refined using successive Fourier maps and full matrix least squares. Parameters refined were the overall scale factors, positional parameters for all atoms, anisotropic thermal parameters for all non-hydrogen atoms, and isotropic thermal parameters for hydrogens. Structural factors for non-hydrogen atoms were taken from the usual source.[26] Metrical features of the ligands themselves agree with previous results on related molecules. As usually observed in crown structures, the aliphatic C–C bonds are shorter (range: from 1.465

(25) Snyder, C. D.; Rapoport, H. *J. Am. Chem. Soc.* **1972**, *94*, 227–231.
(26) *International Tables for X-ray Crystallography*; Kynoch Press: Birmingham, 1974.

Table I. Crystallographic Data for [Li(NCS)·(**1**)], [Na(NCS)·(**1**)], **2**, [Na(NCS)·(**2**)], and [K(NCS)·(**2**)]

cmpnd	[Li(NCS)·(**1**)]	[Na(NCS)·(**1**)]	**2**	[Na(NCS)·(**2**)]·MeCN	[K(NCS)·(**2**)]
formula wt	407.46	423.51	386.49	508.61	483.67
space group	$P2_1/n$ (No. 14)	$P2_1/c$ (No. 14)	$P2_12_12_1$ (No. 19)	$P2_1/c$ (No. 14)	$P2_1/c$ (No. 14)
a, Å	14.103 (4)	10.182 (4)	8.195 (1)	11.308 (1)	17.377 (3)
b, Å	8.493 (4)	8.601 (1)	11.541 (1)	14.521 (2)	10.600 (2)
c, Å	19.128 (8)	25.631 (3)	22.449 (3)	16.440 (4)	27.538 (7)
α, deg	90	90	90	90	90
β, deg	108.70 (9)	97.29 (3)	90	91.56 (1)	102.41 (3)
γ, deg	90	90	90	90	90
V, Å	2170	2227	2123	2698	−4953
d_{calc}, g cm^{-3}	1.24	1.26	1.21	1.25	1.30
d_{obsd}, g cm^{-3}	1.26				
Z	4	4	4	4	8
μ, cm^{-1}	15.62	17.29	7.08	15.45	1.97
final R, %	5.44	7.58	5.58	4.87	8.23
final R_w, %	6.74	7.81	6.64	4.33	9.45

Table II. Selected Bond Lengths (Å) and Angles (deg) for [Li(NCS)·(**1**)]

Li–N	1.972 (5)	Li–O2	2.135 (5)
Li–O5	2.147 (5)	Li–O8	2.048 (4)
Li–O210	2.087 (5)		
N–C	1.151 (3)	S1–C	1.626 (3)
O2–Li–N	117.1 (2)	O5–Li–N	116.8 (2)
O5–Li–O2	77.8 (2)	O8–Li–N	111.2 (2)
O8–Li–O2	131.5 (2)	O8–Li–O5	77.9 (2)
O210–Li–N	101.5 (2)	O210–Li–O2	84.9 (2)
O210–Li–O5	141.7 (2)	O210–Li–O8	89.0 (2)
C–N–Li	163.0 (3)	S1–C–N	179.8 (2)

(6) to 1.502 (6) Å) than expected for C(sp^3)–C(sp^3) bonds. The atomic numbering system used for all of the quinone crowns (as the hydroquinone dimethyl ethers) appears in Figure 1.

For [Na(NCS)·(**1**)], [Na(NCS)·(6QC-HQDME)], and [K(NCS)·(6QC-HQDME)], the observed systematic absences ($h0l$, l odd; $0k0$, k odd; $00l$, l odd) uniquely defined the space group as $P2_1/c$. Systematic absences for [Li(NCS)·(**1**)] ($h0l$, $h + l$ odd, $0k0$, k odd) uniquely indicated space group $P2_1/n$, while those for free 6QC-HQDME ($h00$, h odd; $0k0$, k odd; $00l$, l odd) uniquely indicated space group $P2_12_12_1$. To prevent decomposition of [Na(NCS)·(6QC-HQDME)]·MeCN the crystal was mounted in its mother liquor.

Results

Descriptions of the Structures. General Features. Two structural motifs occur in the complexed ligands. In [Li(NCS)·(5QC-HQDME)],[27] [Na(NCS)·(6QC-HQDME)(MeCN)], and [K(NCS)·(6QC-HQDME)] (molecule A) (see Figure 1) mononuclear complexes contain thiocyanate in an apical position above an idealized MO_n plane, with ∠M–N(CS) angles approaching linearity (>150°). On the other hand, [Na(NCS)·(5QC-HQDME)] and [K(NCS)·(6QC-HQDME)] both crystallize as di-μ-thiocyanato bridged dimers, with ∠M–N–M angles nearer 90°. In either case thiocyanate binds through the N atom. Each complex features strong M–O bonding to the crown ether oxygen atom diametrically opposite the metal ion. Importantly, in each case anisole O atom (O210) coordinates strongly; this interaction couples the redox state of the quinoid group with ion binding by the crown. On the other hand, benzylic O atoms in several complexes bind either weakly or not all. Specific comments follow.

[Li(NCS)·(5QC-HQDME)] contains Li$^+$ bound to five atoms: three of the four crown O atoms, one anisole O atom, and an apical NCS$^-$ group together approximately yield a square-pyramidal array (Figure 2; Table II). Lithium lies 0.77 Å above the irregular square formed by the four O atoms; an angularly bound thiocyanate (∠Li–N–C = 163°) completes the coordination sphere. Benzylic oxygen atom O11 fails to coordinate (Li···O11 = 4.25 Å), apparently because coordination to the small Li$^+$ cation necessitates a "bowl" conformation of the crown loop (cf. the more

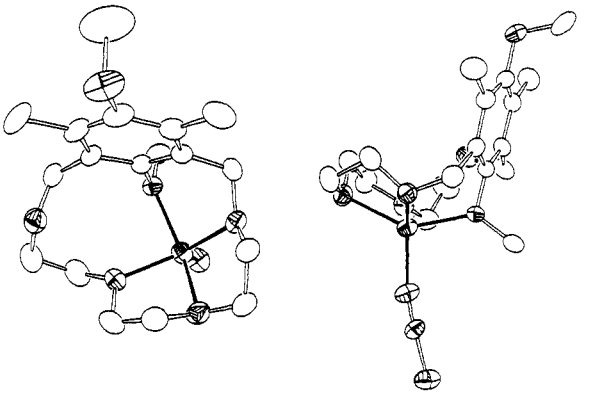

Figure 2. ORTEP diagrams of [Li(NCS)·(5QC-HQDME)] in top and side views.

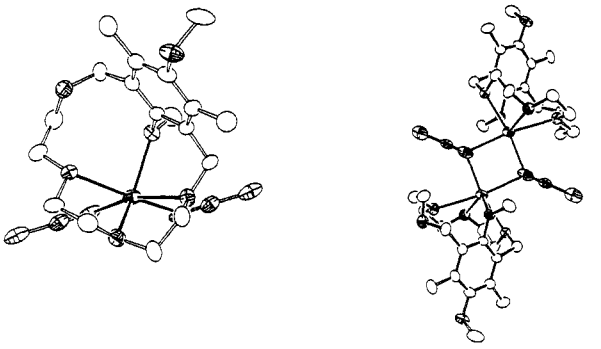

Figure 3. ORTEP diagrams of [Na(NCS)·(5QC-HQDME)]$_2$: (left) top half of dimer, showing detailed geometry and (right) view of full dimer.

usual flat conformation of crown complexes) (e.g., 18-crown-6)[28,29] The "bowl" conformation maximizes Li–O interaction for three of the crown O atoms but effectively precludes it for the fourth, which adopts a position that makes coordination impossible.

Lithium–oxygen distances yield a two long, two short pattern (2.135 (5), 2.147 (5), 2.048 (4), 2.087 (5) Å; Table II) with shorter distances to the anisole O atom (O210) and O8. The average Li–O distance (2.10 Å) slightly exceeds those in [Li(NCS)(16-crown-4)][30] and [Li(12-crown-4)(NCS)][31] (both 2.08 Å), and considerably exceeds that in [Li(dibenzo-14-crown-4)(NCS)] (2.04 Å)[32] and [Li(*cis-syn-cis*-dicyclohexano-14-crown-4)(NCS)].[33] These results and a search of the Cambridge Crystallographic Database indicate that the suggested normal Li–O distance in

(27) Nomenclature used: nQC denotes a quinone crown ether with n ether oxygen atoms (one anisole and $n - 1$ crown O atoms) capable of binding to one metal ion. nQC-HQDME denotes the hydroquinone dimethyl ether of that same quinone crown.

(28) Dunitz, J. D.; Seiler, P. *Acta Crystallogr.* **1974**, *B30*, 2739–2741.
(29) Maverick, E.; Seiler, P.; Schweizer, W. B.; Dunitz, J. D. *Acta Crystallogr.* **1980**, *B36*, 615–620.
(30) Groth, P. *Acta Chem. Scand.* **1981**, *A35*, 460–462.
(31) Groth, P. *Acta Chem. Scand. Ser. A* **1981**, *A35*, 463–465.
(32) Shoham, G.; Lipscomb, W. N.; Olsher, U. *J. Chem. Soc., Chem. Commun.* **1983**, 208–209.
(33) Buchanan, G. W.; Kirby, R. A.; Charland, J. P. *J. Am. Chem. Soc.* **1988**, *110*, 247–2483.

Table III. Selected Bond Lengths and Angles (deg) for [Na(NCS)·(**1**)]

Na–Na	3.611 (3)	Na–O8	2.660 (3)
Na–O5	2.442 (3)	Na–O2	2.454 (3)
Na–N0	2.520 (4)	Na–N0	2.406 (4)
Na–O210	2.412 (3)		
S0–C0	1.623 (5)	C0–N0	1.148 (5)
N0–Na–Na	41.65 (9)	N0–Na–N0	85.8 (1)
N0–C0–S0	179.2 (5)	C0–N0–Na	132.6 (4)
Na–N0–Na	94.2 (1)	C0–N0–Na	129.0 (3)

Table IV. Selected Bond Lengths (Å) and Angles (deg) for Free **2**

O2–C1	1.404 (4)	O2–C3	1.426 (4)
O5–C4	1.401 (4)	O5–C6	1.413 (4)
O8–C7	1.421 (5)	O8–C9	1.414 (4)
O11–C10	1.414 (4)	O14–C15	1.416 (4)
O240–C24	1.399 (4)	O240–C240	1.442 (5)
C1–C26	1.500 (5)	C3–C4	1.474 (6)
C6–C7	1.481 (6)	C9–C10	1.492 (6)
C12–C13	1.489 (6)	C15–C22	1.500 (5)

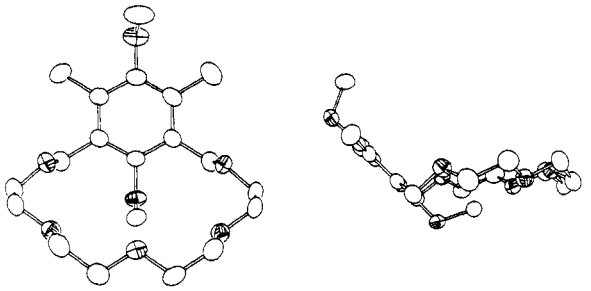

Figure 4. ORTEP diagrams of 6QC-HQDME in top and side views.

five-coordinate macrocyclic complexes[32] (2.04 Å) should probably be revised to 2.08 and 2.13 Å for $LiO_4(NCS)$ and LiO_5 complexes, respectively.[34]

The Li–NCS distance (1.972 (5) Å) compares closely with those in some previously reported [Li(NCS)(L)] complexes (L = 16-crown-4 (1.96 (1) Å)[30] and dibenzo-14-crown-4 (1.96 Å),[32] but it is shorter than those in others (L = 12-crown-4 (2.04 (1) Å)[31] and *cis-syn-cis*-dicyclohexano-14-crown-4 (2.029 (10) Å)).[33]

[Na(NCS)·(5QC-HQDME)] crystallizes as a centrosymmetric dimer with two $^-$*N*CS anions asymmetrically bridging two six-coordinate Na^+ cations (Figure 3; Table III). Two angularly bonded $^-$*N*CS groups bridge the Na^+ ions (d(Na···Na) = 3.611 (3) Å) with substantially different Na–N distances (2.520 (4) and 2.454 (3) Å) to form an Na_2N_2 rhombohedron. The resulting coordination geometry at Na resembles that of a square prism after removal of two atoms related by a face diagonal. As in the Li^+ analogue, each Na^+ coordinates to one benzylic O atom (2.454 (3) Å), but not the other (Na···O11 = 4.53 Å). Each also coordinates to one anisole (Na–O210 = 2.412 (3) Å) and two other crown O atoms (Na–O = 2.660 (3), 2.442 (3) Å) (Figure 3). The four oxygen atoms form an irregular square, with the sodium atom 1.3 Å above their mean plane. As in the analogous Li complex, the ligand here also adopts the "bowl" conformation. The average Na–O distance, 2.49 Å, compares closely with those found for the numerous six-coordinate macrocyclic ether complexes in the Cambridge crystallographic database (2.5 Å).[34] Structurally [Na(NCS)·(5QC-HQDME)]$_2$ resembles [M(NCS)(18-crown-6)] (M = Rb,[35] Cs[36]), which also adopt the di-μ-NCS bridged structure.

6QC-HQDME in its free state (Figure 4; Table IV) approaches mirror symmetry; the anisole methoxyl group (O210–C210) dangles over the crown ring and the methyl group points into the crown cavity, approaching O5, O8, and O11 at distances ranging from 3.2 to 3.3 Å. Association of C–H bonds with ethereal O atoms is a common feature of free crown ethers. Conformationally 6QC-HQDME closely resembles free 18-crown-6.[28,29]

Table V. Selected Bond Angles (Å) for [Na(NCS)·(**2**)]·CH_3CN

Na–O5	2.583 (3)	Na–O210	2.492 (2)
Na–O8	2.482 (2)	Na–O11	2.685 (3)
Na–N1	2.410 (4)	Na–N100	2.477 (4)
Na···O2	2.978 (3)	Na···O14	3.386 (3)
C101–C100–N100	179.6 (4)	C100–N100–Na	150.7 (3)
S1–C200–N1	179.9 (4)	C200–N1–Na	157.2 (3)

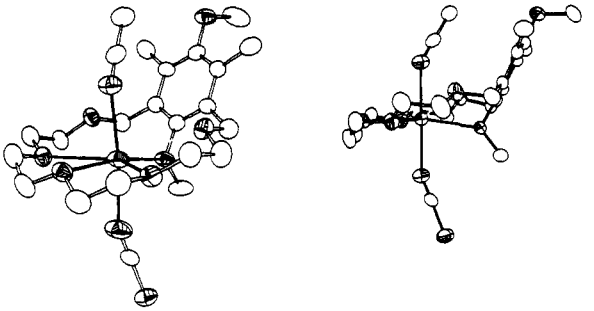

Figure 5. ORTEP diagrams of [Na(NCS)·(6QC-HQDME)·(MeCN)] in oblique and side views.

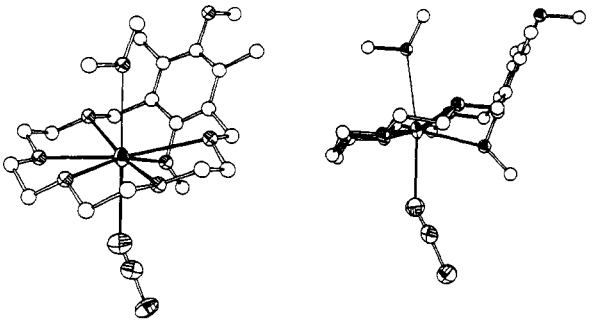

Figure 6. ORTEP diagrams of [K(NCS)·(6QC-HQDME)] (molecule A) in oblique and side views.

[Na(NCS)·(6QC-HQDME)]·CH_3CN results from addition of NaNCS to a solution of 6QC-HQDME in CH_3CN and contains a six-coordinate Na^+ ion essentially within the plane of the crown ligand (Figure 5; Table V). An anisole and three crown O atoms coordinate at short distances (Na–O(anisole) = 2.492 (2) Å; Na–O(crown) = 2.583 (3), 2.482 (2), and 2.685 (3) Å); neither benzylic O atom coordinates (Na···O = 2.978 (3) and 3.386 (3) Å). Two axially disposed N atoms, one each from an $^-$*N*CS group and from a CH_3CN of crystallization (Figure 5), coordinate on opposite sides of the idealized NaO_4 plane (Na–N = 2.410 (4) and 2.477 (4) Å, respectively), from which the Na protrudes by 0.19 Å. Both Na–N–C units deviate substantially from linearity (∠Na–N–C = 157° and 150 for the NCS and NCMe groups, respectively). The resulting Na coordination sphere approaches octahedral geometry. Sodium–oxygen distances average 2.56 Å, and therefore somewhat exceed the average found for six-coordinate complexes of macrocyclic ethers in the Cambridge Crystallographic Database (2.5 Å),[34] but agree well with those found for, e.g., [Na(NCS)(18-crown-6)(OH_2)] (2.55 Å).[37]

Two molecules comprise the asymmetric unit of [K(NCS)·(6QC-HQDME)], a monomeric complex and half of a dimer. The monomeric complex (molecule A) resembles [Na(NCS)·(6QC-HQDME)]; it has an essentially flat crown loop with the K^+ ion approximately in the plane of the macrocyclic ring with two apical

(34) Supplementary material.
(35) Dobler, M.; Phizackerley, R. P. *Acta Crystallogr.* **1974**, *B30*, 2746–2748.
(36) Dobler, M.; Phizackerley, R. P. *Acta Crystallogr.* **1974**, *B30*, 2748–2750.
(37) Dobler, M.; Dunitz, J. D.; Seiler, P. *Acta Crystallogr.* **1974**, *B30*, 2741–2743.

Table VI. Selected Bond Lengths (Å) and Angles (deg) for [K(NCS)·(2)]

molecule A		molecule B	
Ka–O2a	2.924 (7)	Kb···O2b	3.311 (8)
Ka–O5a	2.750 (8)	Kb–O5b	2.899 (9)
Ka–O8a	2.753 (8)	Kb–O8b	2.804 (10)
Ka–O11a	2.749 (7)	Kb–O11b	2.917 (8)
Ka–O14a	3.014 (7)	Kb···O14b	3.202 (7)
Ka–O210a	2.612 (8)	Kb–O210b	2.725 (8)
Ka–O240a′	3.100 (9)	Kb–O240b	3.311 (8)
Ka–N0a′	2.897 (13)	Kb–N0b	2.823 (11)
		N0b–Kb′	2.816 (9)
		Kb···Kb′	4.248 (5)
S0a–C0a	1.614 (15)	Sb–C0b	1.652 (12)
N0a–C0a	1.142 (19)	N0b–C0b	1.135 (15)
C0a–N0a–Ka′	151.10 (10)	C0b–N0b–Kb′	128.4 (8)
S0a–C0a–N0a	176.1 (12)	Sb–C0b–N0b	178.0 (11)
		N0b–Kb′–N0b′	82.3 (3)
		Kb–N0b′–Kb′	97.7 (3)
		N0b–Kb–Kb′	41.1 (2)
		N0b–Kb–N0b′	82.3 (3)
		Kb–N0b–C0b	129.5 (9)
		Kb–N0b–Kb′	97.7 (3)

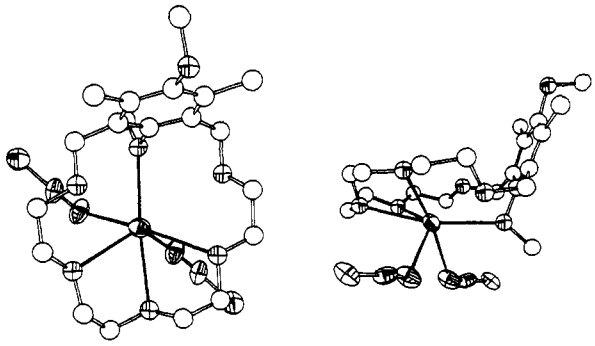

Figure 7. ORTEP diagrams of [K(NCS)·(6QC-HQDME)] (molecule B) in oblique and side views of half of the dimeric complex.

substituents (Figure 6; Table VI). Seven atoms bind the K^+ ion in a distorted pentagonal bipyramid; one anisole (K–O210 = 2.612 (8) Å), three crown (K –O = 2.749 (7), 2.753 (8), and 2.750 (8) Å), and two benzylic O atoms (K–O = 2.924 (7) and 3.014 (7) Å) coordinate equatorially, while an $^-$NCS (2.897 (13) Å; ∠KNC = 151°) binds axially. In addition, an anisole group from another molecule (K–O240′ = 3.100 (9) Å) interacts weakly from just beyond a bonding distance.

In molecule B [K(NCS)·(6QC-HQDME)] units interact via two bridging $^-$NCS groups (K···K = 4.248 (5) Å), with d(K–N) = 2.823 (11) and 2.816 (9) Å (∠K–N–C = 130 and 128°) to yield a dimer similar to [Na(NCS)·(5QC-HQDME)]$_2$ (Figure 7; Table VI) and [M(NCS)(18-crown-6)] (M = Rb,[35] Cs[36]). The six-coordinate potassium ion also bonds to one anisole (2.725 (8) Å) and three crown O atoms (2.899 (9), 2.804 (10), and 2.917 (8) Å) to give an irregular coordination sphere. (Neither benzylic O atom bonds: K···O = 3.311 (8) and 3.202 (7) Å). Potassium–oxygen distances in molecules A and B average 2.80 and 2.84 Å, respectively, compared with a value of 2.8 Å found in the Cambridge Crystallographic Database[34] and 2.80 Å found for [K(NCS)(18-crown-6)].[38] The potassium ion lies out of the crown plane (by 1.64 Å) toward the anisole and bridging NCS groups. Conformationally molecule B features a "bowl" conformation more similar to those in [M(NCS)·(5QC-HQDME)] (M = Li, Na) than those in [Na(NCS)·(6QC-HQDME)·(MeCN)] or molecule A.

Electrochemical Studies. In the absence of metal cations all of the quinone crowns undergo two quasi-reversible reductions in DMF near –0.61 and –1.58 V (vs SCE), corresponding to the

Table VII. Formal Reduction Potentials (V vs SCE) for Quinone Crowns in the Presence of Group I Cations (0.1 M M^+ as Tosylate or Tetraphenylborate)

compd	cation	E_0	ΔE (mV)[a]	binding enhancement
Me_2BMBQ	free	–0.604		
	Li	–0.574	28	3
	Na	–0.592	9	1
	K	–0.598	4	1
	Rb	–0.599	2	1
	Cs	–0.599	2	1
5QC	free	–0.615		
	Li	–0.549	66	13
	Na	–0.547	68	14
	K	–0.547	68	14
	Rb	–0.548	67	13
	Cs	–0.555	60	10
6QC	free	–0.622		
	Li	–0.570	56	7
	Na	–0.496	130	156
	K	–0.466	162	542
	Rb	–0.488	138	213
	Cs	–0.510	117	94
7QC	free	–0.614		
	Li	–0.576	38	4
	Na	–0.546	68	14
	K	–0.508	106	61
	Rb	–0.500	114[b]	84
	Cs	–0.482	132	168
8QC	free	–0.609		
	Li	–0.575	33	3
	Na	–0.542	67	13
	K	–0.536	74	17
	Rb	–0.522	87	29
	Cs	–0.518	91	36

[a] Calculated as $E_{complex} - E_{free}$. [b] Calculated from the reduction wave only due to broadening of the oxidation wave.

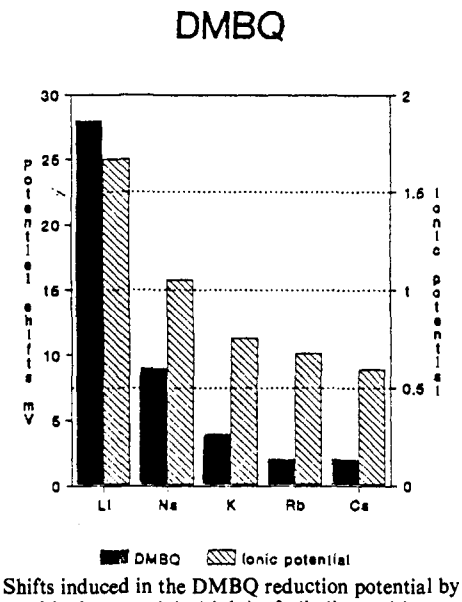

Figure 8. Shifts induced in the DMBQ reduction potential by 0.1 M M OTs (left) and ionic potentials (right) of alkali metal ions.

quinone/semiquinone radical anion (Q/SQ^-) and semiquinone radical anion/hydroquinone dianion (SQ^-/HQ^{2-}) couples, respectively (Table VII). Unlike quinoid species examined in MeCN, those reported here show only a single wave in the presence of cations (instead of separate waves for the bound and free forms).[39] Cation-induced shifts in the SQ^-/HQ^{2-} couple differ little between quinone crowns and 2,6-bis(methoxymethyl)-3,5-dimethyl-1,4-benzoquinone (Me_2BMBQ), whose shifts result solely from ion pairing. Further discussion is limited to

(38) Seiler, P.; Dobler, M.; Dunitz, J. D. *Acta Crystallogr.* **1974**, *B30*, 2744–2745.

(39) Miller, S. R.; Echegoyen, L.; Chen, Z. H.; Gustowski, D. A.; Kaifer, A. E.; Gokel, G. W. *Anal. Chem.* **1988**, *60*, 2021–2024.

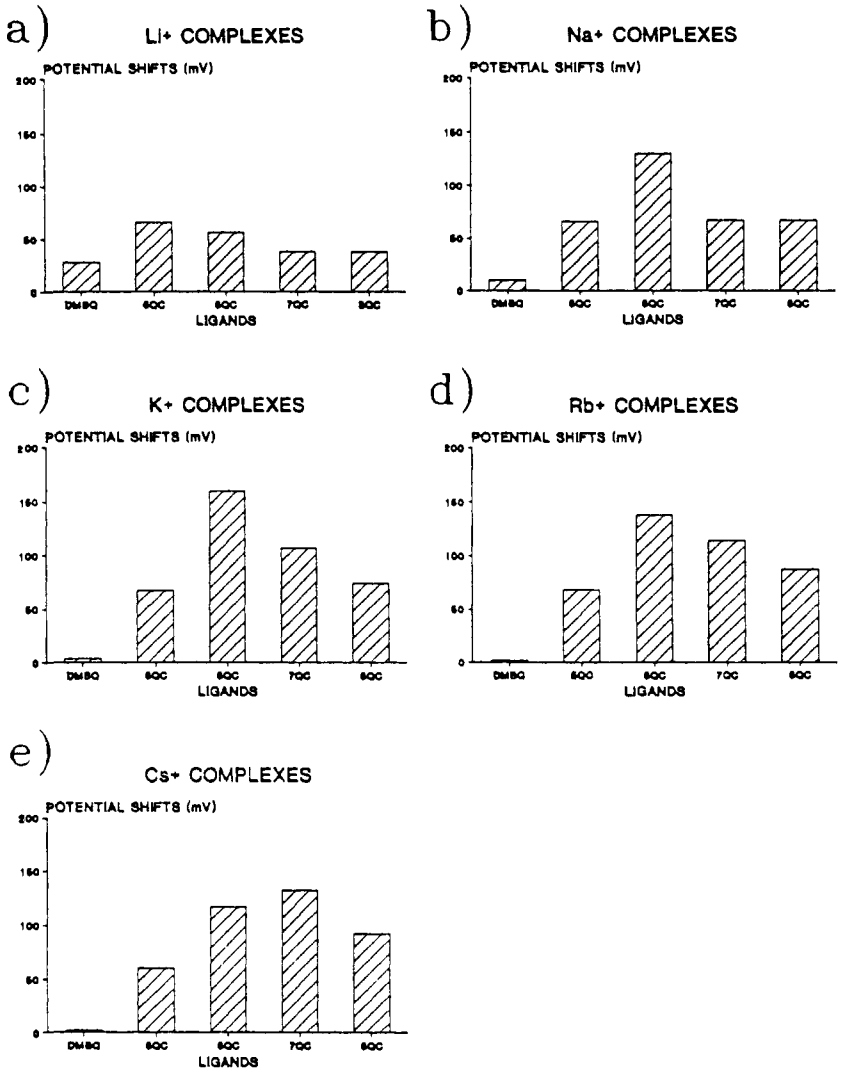

Figure 9. Electrochemical shifts of quinone crowns (5-8 QC) in the presence of 0.1 M alkali metal tosylates.

the Q/SQ^- couples, since only they show specific complexation effects.

Alkali metal tosylates (0.1 M) anodically shift the Q/SQ^- potential of 2,6-bis(methoxymethyl)-3,5-dimethyl-1,4-benzoquinone with progressively smaller magnitude from Li^+ to Cs^+ (28 to 3 mV). These results parallel the pattern in charge/size ratio ($r_{ionic}(Li^+)$ = 0.76 Å; $r_{ionic}(Cs^+)$ = 1.67 Å)[40] (Table VII; (Figure 8). They are consistent with simple ion pairing and minimal complexation; Me_2BMBQ therefore represents a control for ion-pairing effects in the quinone crowns.

Lithium induces anodic shifts that decrease from 5QC (66 mV) (Figure 9a) to 6QC (56 mV) and finally approach the ionic pairing limit for 7- and 8QC (38 and 35 mV), respectively (cf. 28 mV for Me_2BMBQ). This trend follows Coulombic interactions between SQ^- and M^+, with the strongest interaction occurring with the ion of greatest ionic potential, Li^+. Since the quinone form binds negligibly,[3] the electrochemical data indicate that the various crown loops differ relatively little in their ability to complex lithium.

Sodium, potassium, and rubidium all induce qualitatively similar potential shifts (Figure 9b–d). In each case 6QC shows the greatest anodic shift in E_t, and hence the greatest increase in binding constant upon reduction. Anodic shifts diminish in magnitude with an increase in ring size (7QC, 8QC) and generally more rapidly with a decrease (5QC). The maximum anodic shift occurs in the K^+/6QC system (162 mV), but all shifts substantially exceed those arising from ion pairing (as represented by the M^+–2,6-bis(methoxymethyl)-3,5-dimethyl-1,4-benzoquinone systems). Cesium displays a different trend; the maximum shift (132 mV) moves from 6QC to 7QC, with greater decrease toward larger ring sizes (8QC, 91 mV) than smaller (6QC, 117 mV) (Figure 9e).

Consideration of the potential shifts as a function of metal ion, rather than ligand, reveals that 5QC shows nearly the same shift for all metal ions (Figure 9a). Correction for ion-pairing (ΔE_{corr} = ΔE(QC) – ΔE(Me_2BMBQ) shows that Li^+ causes the smallest shift arising only from complexation. Shifts with 6QC display a clear maximum at K^+ (Figure 9b), while those for 7- and 8QC attain their maximum value with Cs^+ (Figure 9c,d).

EPR Studies. In the absence of cations electrogenerated semiquinone crowns yield essentially identical EPR spectra, with proton hyperfine couplings to six equivalent methyl ($a(CH_3)$ = 2.05 G) and four equivalent benzylic methylene protons ($a(CH_2)$ = 0.71 G) (Table VIII).

Lithium cations perturb both the electron and the spin density in semiquinones. In electrochemically-reduced Me_2BMBQ Li^+ only broadens the lines, but with reduced 5QC Li^+ increases ^1H coupling constants ($a(CH_3)$ = 2.85 G and $a(CH_2)$ = 0.72 G), a reflection of greater spin density localization at these positions. Similar shifts occur in reduced 6QC ($a(CH_3)$ = 2.69 G and $a(CH_2)$ = 0.46 G), but with smaller spin density at the methylene positions. Electrochemically-reduced 7- and 8QC behave analogously. No semiquinone crown exhibits superhyperfine splitting from ^7Li, despite high charge density and large nuclear magnetic moment of the predominant isotope (^7Li, 92.58%, $I = {}^3/_2$, μ = +3.2564 μ_N).

(40) Shannon, R. D. *Acta Crystallogr.* **1976**, *A32*, 751–767.

Table VIII. EPR Coupling Constant[a] of Electrochemically Reduced Quinone Crowns in the Presence of 0.1 M M(OTs)

compd	coupling	free	Li	Na	K
Me_2BMBQ	$a(CH_3)$	2.04[a]	b	2.17	2.14
	$a(CH_2)$	0.71	b	0.67	0.68
	$a(M^+)$				
5QC	$a(CH_3)$	2.07	2.85		2.25
	$a(CH_2)$	0.49	0.72		1.03
	$a(M^+)$				
6QC	$a(CH_3)$	2.06	2.69	2.35	2.39
	$a(CH_2)$	0.83	0.46	0.78	0.83
	$a(M^+)$			0.92	
7QC	$a(CH_3)$	2.07	2.71	2.6	2.37
	$a(CH_2)$	0.75	0.72	0.5	0.48
	$a(M^+)$				
8QC	$a(CH_3)$	2.03	3.1		2.38
	$a(CH_2)$	0.73	0.7		0.45
	$a(M^+)$				

[a] In G. [b] Broad.

Sodium cations only slightly perturb the EPR spectrum of electrochemically-reduced Me_2BMBQ ($a(CH_3)$ = 2.17 G and $a(CH_2)$ = 0.67 G). By contrast, Na^+ coordination to semiquinone crowns significantly changes ^1H hyperfine coupling constants ($a(CH_3)$ increases and $a(CH_2)$ decreases (Table VIII)). ^{23}Na superhyperfine splitting ($a(^{23}Na)$ = 0.92 G) appears only in reduced 6QC;[8] its absence with other semiquinone crowns may result from their suboptimal fit for this cation, with concomitant diminution of M–SQ interaction.

Potassium salts added to electrochemically reduced Me_2BMBQ yield an EPR spectrum ($a(CH_3)$ = 2.14 G and $a(CH_2)$ = 0.67 G) similar to that obtained with Na^+. Semiquinone crowns hyperfine coupling increases at both the methyl and the benzylic methylene positions, the latter more so than the former (for reduced 5QC $a(CH_3)$ = 2.25 G and $a(CH_2)$ = 1.03 G); reduced 6-, 7-, 8QC behave similarly. No ligand revealed resolved K^+ superhyperfine splitting, presumably because of the small nuclear magnetic moment of potassium (^{39}K, 93.1%, $I = {}^3/_2$, μ = +0.3914 μ_N).

Discussion

Several conclusions emerge from this work. First, as reflected in M–O distances, benzylic oxygen atoms provide suboptimal coordination, especially in the Na^+ and K^+ complexes of 6QC-HQDME. In complexes of 5QC-HQDME one benzylic O atom coordinates at a distance comparable to those of aliphatic donors. In contrast, in complexes of 6QC-HQDME the benzylic ether groups bind weakly, if at all, at distances >0.2 Å longer than those to aliphatic donors.

Comparison of free 6QC-HQDME with 18-crown-6[28,29] suggests that inclusion of the quinoid ring minimally perturbs the ring conformation. In crown conformation free 6QC-HQDME, [Na(NCS)·(6QC-HQDME)(MeCN)], and [K(NCS)·(6QC-HQDME)] (molecule A) all closely resemble free 18-crown-6 (although [K(NCS)·(6QC-HQDME)] (molecule B) differs considerably). Torsional angles of the crown loops of [M(NCS)·(5QC-HQDME)] (M = Li, Na)[34] parallel each other closely except at the unbound portion of the ring.

Of especial interest in these structures is the efficacy of the metal–anisole interaction. In all cases anisole oxygen atoms are among the strongest binding groups. Proximity to the aromatic ring may enhance the donor properties of the anisole group and thereby favor its coordination. Stronger coordination to the anisole group may weaken interaction with the benzylic ethers, or vice versa.

The quinoid moiety pivots to allow optimal M–O interaction. Non-bonded O···O distances between anisole-type donor O210 and the adjacent benzylic O atoms (O2 and either O11 (for 5QC-HQDME) or O14 (for 6QC-HQDME)) decrease from those of free 6QC-HQDME (O···O(av) = 3.43 Å) upon coordination to Na^+ (3.03 and 3.10 Å) or K^+ ((3.13 and 3.08 Å for molecule A; 3.26 and 2.96 Å for molecule B). Similar effects occur in complexes of 5QC-HQDME. In [Li(NCS)·(5QC-HQDME)] the O210···O2 and O210···O11 distances are 2.85 and 3.54 Å, respectively. Similarly, O···O distances in [Na(NCS)·(5QC-HQDME)] and O210···O2 are 3.03 and 3.49 Å. Pivoting by the quinoid moiety allows it to accommodate metal ions of varying sizes, and thereby precludes any significant contribution to metal ion selectivity.

Coupling between ion binding and redox state stabilizes semiquinone relative to quinone crowns in the presence of metal ions, and thereby shifts reduction potentials to more reducing values. Stabilization results not only from complexation, however, but also from simple ion-pairing, which lacks specificity and therefore is not of interest in this context. To minimize ion-pairing effects the present electrochemical measurements were performed in DMF, and potential shifts are reported in comparison with those of Me_2BMBQ. The reported shifts represent a lower bound; use of MeCN, for example, yields considerably larger shifts, under essentially the same conditions,[19] largely because it does not suppress ion-pairing as effectively as DMF. In addition, because MeCN solvates anions and possibly cations less effectively than DMF, it enhances the apparent binding constants of both oxidized and reduced forms and thereby generates two-wave behavior for the Q/SQ^- couple (instead of one wave that shifts with $[M^{n+}]$, as observed here).

Thermodynamically, complex formation shifts Q/SQ^- reduction potentials according to

$$E_f = E_0 - RT/nF \ln \{\alpha^Q/\alpha^{SQ}\} \quad (1)$$

where α^{SQ} is the partition function for the SQ form ($\alpha^{SQ} = 1 + K^{SQ}_{1/2}[M^{1/2} + K^{SQ}_1[M] + K^{SQ}_1K^{SQ}_2[M]^2 + \cdots$, for 0:1, 2:1, 1:1, and 1:2 complexes with cation M, respectively), and similarly for α^Q. Complete formation of the 1:1 complexes would simplify this equation to

$$E_f = E_0 - RT/{}_nF \ln \{K^Q/K^{SQ}\} \quad (2)$$

the form in which data have previously been interpreted, where binding enhancement factors attendant upon reduction were calculated from the ΔE induced by addition of a metal salt. Miller et al.,[39] however, have recently shown that such calculations based upon cyclic voltammetric data can seriously underestimate binding enhancements when the oxidized form binds weakly (i.e., the ox/red couple exhibits only one wave that continuously shifts in potential as a function of $[M^{n+}]$, instead of two that vary in current), as in the present case. This is because the cyclic voltammetric process corresponds not to a simple reduction but rather to an EC process, and the cyclic voltammetric peak currents reflect the kinetics of complexation, which of course also depend on $[M^{n+}]$.

With this caveat, reduction potentials (Table I) show that 6QC exhibits the greatest anodic shift with most of the cations. Unlike previously reported redox-active crowns, 6QC provides the greatest shift with K^+, followed by Rb^+, Na^+, Cs^+, and Li^+. The electrochemical data show that cation binding results primarily from coordination by the macroring and not ion pairing. Potential shifts decrease in the order $K^+ > Rb^+ > Na^+ > Cs^+ > Li^+$; ion pairing strength follows charge to radius ratio, and hence Li^+ would show the greatest, rather than the smallest, anodic shift. Consequently, ion pairing plays a minor role compared to macrocyclic coordination in determining the potential shifts.

Conclusions

Structural studies of the quinoid crowns show the following: (1) in all structures the anisole group binds strongly, as does the crown O atom diametrically opposite to it; (2) benzylic ether groups generally bind weakly; (3) in 6QC complexes incorporation of the *m*-xylyl group minimally perturbs the crown conformation from that of the corresponding complex of 18-crown-6; and (4) the quinoid moiety pivots to accommodate metal ions of differing size and as a consequence metal ion selectivity arises solely from the crown loop. Owing to the last point, efforts devoted to enhancing the metal ion discrimination of the quinone crowns must necessarily focus upon the crown loop by restricting it conformationally. Work to this end will be reported subsequently.

Electrochemical studies show that incorporation of quinone groups into crown ethers couples redox reactions with binding of group IA cations. In contrast to expectations from ion pairing, K^+ with 6QC yields the largest potential shift, followed by $Rb^+ > Na^+ > Cs^+ > Li^+$. Structural studies show that the observed ion selectivity derives from the crown loop, not the quinoid moiety, owing to the latter's ability to pivot with respect to the macrocycle plane and thereby to accommodate a range of cations. EPR studies demonstrate the intramolecular nature of interaction between the cations and the ligands. In its semiquinone form only 6QC shows a metal hyperfine coupling constant with Na.

Acknowledgment. We are grateful to the donors of the Petroleum Research Fund, administered by the American Chemical Society, to Medisense (U.K.), and to the Science and Engineering Research Council (U.K.) for support of this research.

Supplementary Material Available: Tables of atomic coordinates, bond angles, bond lengths, anisotropic thermal parameters, hydrogen atomic positions, and torsional angles, and an outline of the searches of the Cambridge Crystallographic Database (52 pages); listing of structure factor tables (69 pages). Ordering information is given on any current masthead page.

Synthesis and Characterization of $Cp_2Zr(CH\{Me\}\{6\text{-ethylpyrid-2-yl}\})(CO)^+$, a d^0 Metal Alkyl Carbonyl Complex. Coordination Chemistry of the Four-Membered Azazirconacycle $Cp_2Zr(\eta^2\text{-}C,N\text{-}CH\{Me\}\{6\text{-ethylpyrid-2-yl}\})^+$

Anil S. Guram, Dale C. Swenson, and Richard F. Jordan*

Contribution from the Department of Chemistry, University of Iowa, Iowa City, Iowa 52242.
Received May 4, 1992

Abstract: The cationic complex $Cp_2Zr(CH_3)(THF)^+$ (**1**, as the BPh_4^- salt) reacts with 2,6-diethylpyridine to afford the chelated secondary zirconocene–alkyl complex $Cp_2Zr(\eta^2\text{-}C,N\text{-}CH\{Me\}\{6\text{-ethylpyrid-2-yl}\})^+$ (**2**). Treatment of complex **2** with CO, CH_3CN, ^tBuCN, and $(PhCH_2)(Et)_3N^+Cl^-$ affords $Cp_2Zr(CH\{Me\}\{6\text{-ethylpyrid-2-yl}\})(CO)^+$ (**3**), $Cp_2Zr(CH\{Me\}\{6\text{-ethylpyrid-2-yl}\})(CH_3CN)^+$ (**4**), $Cp_2Zr(CH\{Me\}\{6\text{-ethylpyrid-2-yl}\})(^tBuCN)^+$ (**5**), and $Cp_2Zr(CH\{Me\}\{6\text{-ethylpyrid-2-yl}\})(Cl)$ (**6**), respectively. The thermally sensitive d^0 carbonyl complex **3** is a rare example of a d^0 M(alkyl)–CO adduct and is unambiguously characterized in solution by low-temperature NMR and IR spectroscopy, ^{13}C-labeling and hydrolysis experiments, and decomposition studies. IR and NMR data establish that **3** contains a terminal CO ligand. An X-ray structure analysis of **6** establishes that the CH(Me)(6-ethylpyrid-2-yl) ligand adopts a chelated structure; the similarity of the spectroscopic data for **3–6** implies that **3–5** have similar chelated structures. At room temperature, **3** in CD_2Cl_2 rapidly decomposes to afford a complex mixture of products. ^1H NMR monitoring of the decomposition of **3** reveals formation of a transient cationic zirconocene–acyl intermediate **9**, which undergoes 1,2-H shift to afford a mixture of isomeric/oligomeric zirconocene–enolates. Treatment of this mixture with $(PhCH_2)(Et)_3N^+Cl^-$ affords $Cp_2Zr(OCH{=}C\{Me\}\{6\text{-ethylpyrid-2-yl}\})Cl$ (**10**) as a mixture of *E*/*Z* isomers, establishing the presence of zirconocene–enolate species. Hydrolysis of the decomposition products of **3** affords a mixture of thermally sensitive tautomers, enol **11**/aldehyde **11'**, which are characterized by NMR, FTIR, and mass spectroscopy.

Introduction

It is generally assumed that the insertion reactions of d^0 metal alkyl and hydride complexes with CO, olefins, and related π-acid substrates involve initial coordination of substrate to the metal center (e.g., eq 1). However the intermediate $L_nM(R)$(substrate) adducts are rarely observed and are presumed to be unstable due to the lack of conventional $d \rightarrow \pi^*$ back-bonding and the rapidity of the subsequent insertion reactions.[1] The characterization of these elusive species is of fundamental importance for understanding the scope and selectivity of insertion reactions and for the design of new reactive organometallic complexes.

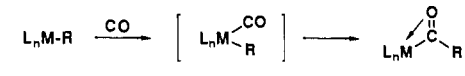

There are few well-characterized d^0 metal–carbonyl complexes. The thermally sensitive $Cp^*_2M(H)_2(CO)$ adducts (M = Zr, Hf) (Chart I) are formed by carbonylation of $Cp^*_2ZrH_2$ at low temperature, and they undergo CO reduction processes when warmed.[2] These complexes exhibit ν_{CO} bands which are decreased by ca. 100 cm^{-1} from that of free CO (Zr 2044, Hf 2036, vs 2143 cm^{-1} for free CO). The low ν_{CO} values are surprising for d^0 complexes and were ascribed to back-bonding form the b_1 M–H bonding MO (antisymmetric combination of the M–H bonds)[3] to the in-plane CO π^*-orbital.[4] In contrast, ν_{CO} values for M–CO complexes in which only σ-donation is important are higher than the free CO value: e.g., H_3BCO 2165 cm^{-1},[5] $Ag(CO)B(OTeF_5)_4$ 2204

Chart I

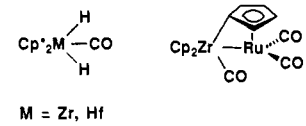

M = Zr, Hf

(1) For selected low-temperature studies of insertion reactions of d^0 alkyls, see: (a) Erker, G. *Acc. Chem. Res.* **1984**, *17*, 103. (b) Erker, G.; Rosenfeldt, F. *Angew. Chem., Int. Ed. Engl.* **1978**, *8*, 605. (c) Burger, B. J.; Thompson, M. E.; Cotter, W. D.; Bercaw, J. E. *J. Am. Chem. Soc.* **1990**, *112*, 1566. (d) Watson, P. L.; Parshall, G. W. *Acc. Chem. Res.* **1985**, *18*, 51. (e) Fagan, P. J.; Moloy, K. G.; Marks, T. J. *J. Am. Chem. Soc.* **1981**, *103*, 6959.

(2) (a) Manriquez, J. M.; McAlister, D. R.; Sanner, R. D.; Bercaw, J. E. *J. Am. Chem. Soc.* **1978**, *100*, 2716. (b) Manriquez, J. M.; McAlister, D. R.; Sanner, R. D.; Bercaw, J. E. *J. Am. Chem. Soc.* **1976**, *98*, 6733. (c) Marsella, J. A.; Curtis, J. C.; Bercaw, J. E.; Caulton, K. G. *J. Am. Chem. Soc.* **1980**, *102*, 7244. (d) Roddick, D. M.; Fryzuk, M. D.; Seidler, P. F.; Hillhouse, G. L.; Bercaw, J. E. *Organometallics* **1985**, *4*, 97.

(3) Lauher, J. W.; Hoffmann, R. *J. Am. Chem. Soc.* **1976**, *98*, 1729.

(4) See ref 2c and Brintzinger, H. H. *J. Organomet. Chem.* **1979**, *171*, 337.

0002-7863/92/1514-8991$03.00/0